Characterization of Alanine-Rich Peptides, Ac-(AAKAA)$_n$-GY-NH$_2$ (n = 1−4), Using Vibrational Circular Dichroism and Fourier Transform Infrared. Conformational Determination and Thermal Unfolding†

Gorm Yoder, Petr Pancoska, and Timothy A. Keiderling*

Department of Chemistry, University of Illinois at Chicago, 845 West Taylor Street (M/C 111), Chicago, Illinois 60607-7061

Received June 18, 1997; Revised Manuscript Received September 8, 1997⊗

ABSTRACT: Vibrational circular dichroism (VCD) and Fourier transform IR (FTIR) were measured for a series of short alanine-based peptides having the general formula Ac-(AAKAA)$_n$-GY−NH$_2$ (n = 1−4) from 5 to 50 °C in D_2O and at room temperature in both TFE and H_2O. In both of these latter solvents, the dominant structural form at the lowest temperature for the longest oligomers is α-helical. The same is true for the n = 4 peptide in D_2O, but under these more dilute aqueous conditions, the shorter (n = 3) peptides have mixed helix−coil structures and the n = 1 and 2 peptides are random coils. The VCD data do not support the 3_{10}-helix as a dominant contributor to the conformation of these oligomers in any of these solvents. These vibrational spectral data are consistent with lower-concentration electronic CD results and additionally indicate increased helical stability at higher concentrations. VCD amide I data for the 22mer (n = 4) in D_2O indicate that the peptide undergoes a transition from a highly helical conformation at 5 °C to a dominant random coil structure at ∼45 °C with a T_m of ∼25 °C (effective midpoint). Factor analysis of the thermal data showed that three principal components were required to describe both the VCD and FTIR data for the n = 4 peptide in D_2O. The transition is characterized by a gradual loss of contribution from a spectral component representing the α-helical fraction. The third component is evidence of an optically detected intermediate conformation best viewed as a mixed coil−helix structure resulting from end fraying of the helical peptide as the temperature is increased. The nature of the junction between the interior helix and frayed ends is not determined by these data and could involve local (ϕ and ψ) angles mimicking a 3_{10}-helix that would provide consistency with ESR and NMR results from Millhauser and co-workers.

The mechanisms contributing to helix formation for peptides and proteins in water have been subjects of considerable interest that is ultimately aimed at gaining a better understanding of the important factors in the protein folding process. These processes have often been characterized by spectroscopic or thermodynamic study of helix formation of peptides of defined length and sequence, with the hope that such specific structural studies might model the early stages of the global protein folding problem (Scholtz & Baldwin, 1992, and references therein). The peptide species studied have been based on both fragments from actual protein sequences and products of *de novo* design. The former are used to explore the relationship between the isolated peptide conformation and that present in the intact protein from which it was derived. With a few notable exceptions such as the C and S peptides from RNase A (Brown & Klee, 1971), such a protein-based approach often does not provide well-formed helices in isolation since the tertiary structure can play a crucial role in initiating and stabilizing helix formation in the native protein. Peptides resulting from *de novo* design, on the other hand, can provide controlled insight into the factors important for helix formation, and allow better probing of the intrinsic helix propensities of the various amino acid sequences. Through design, they can be made relatively free of problems associated with aggregation and peptide−peptide interactions.

An extensive body of research has developed following the demonstration of Marqusee et al. (1989) that peptides of only moderate length containing a high fraction of Ala residues have a relatively high fraction of helix formation at low temperatures as judged by their electronic (UV) circular dichroism (ECD)[1] spectral band shapes. These designed sequences interspersed Ala with charged residues to maintain solubility while inhibiting aggregation. Alternate versions used salt bridges to stabilize specific forms (Marqusee & Baldwin, 1987; Merutka & Stellwagen, 1990; Lyu et al., 1989; Perutz & Fermi, 1988). While considerable data have arisen with regard to various factors that stabilize such helical formation in water, including length effects (Scholtz et al., 1991a; Rohl et al., 1992), it remained clear that these peptides were exceptionally stable, particularly with respect to the helix stability predictions of Zimm−Bragg theory using parameters determined from "host−guest" experiments (Scholtz et al., 1992; Zimm & Bragg, 1959). More recently, the field was given a new twist in a series of papers from

†The work at UIC was supported by a grant from the National Institutes of Health (GM30147).

* To whom correspondence should be addressed.

⊗ Abstract published in *Advance ACS Abstracts,* November 15, 1997.

[1] Abbreviations: $\mathbf{C}_{ij}$, matrix of principal component loadings; ECD, electronic circular dichroism; ESR, electron spin resonance; FA, factor analysis; FTIR, Fourier transform infrared; NMR, nuclear magnetic resonance; PC/FA, principal component method of factor analysis; $\phi_i(\nu)$, principal component spectra; S/N, signal-to-noise ratio; $\theta_j(\nu)$, experimental spectra; $R = \theta_{222}/\theta_{208}$, ratio of CD ellipticities as a test of 3_{10}- vs α-helix; TFA, trifluoroacetic acid; TFE, trifluoroethanol; UV, ultraviolet; VCD, vibrational circular dichroism.

S0006-2960(97)01460-8 CCC: $14.00

Millhauser and co-workers (Hanson et al., 1996a,b; Millhauser, 1995; Martinez & Millhauser, 1995; Fiori et al., 1993; Miick et al., 1991, 1992, 1995) which provided evidence of the possibility of some of these peptides being at least partially in a 3_{10}-helical conformation, particularly the shorter ones (Millhauser, 1995; Miick et al., 1992, 1995). Additionally, even longer peptides were proposed to undergo an α-helix to 3_{10}-helix transformation as they were heated before eventually assuming a high-temperature coil form (Millhauser, 1995; Miick et al., 1995). These data depend on substitution of selected residues of the helix with spin probes either bound to substituted Cys residues or as part of specific, 3_{10}-helix-promoting residues. Various studies of this group indicate that very short oligopeptides (hexamers) are predominantly 3_{10}-helical, including crystal structure data (Toniolo et al., 1995), and longer ones have a mixed α- and 3_{10}-helical conformation with the balance between these conformational types changing with length. Later studies by this group have refined the description of this mix so it is expected to be characterized by α-helical central domains with 3_{10}-helical ends. Studies from this and other groups have indicated the longer helix-forming peptides are most stable in the middle and next at the N terminus which is consistent with their unfolding by fraying from the ends rather than via a two-state cooperative transition (Rohl & Baldwin, 1994; Rohl et al., 1992; Scholtz et al., 1991a; Millhauser, 1995; Todd & Millhauser, 1991; Miick et al., 1991, 1993, 1995). Just as this paper was being finalized for submission, Millhauser et al. (1997) published a new, quite detailed NMR study of a modified Ala-rich 16mer peptide sequence that provided data which could be interpreted in terms of the relative contributions of 3_{10}- to α-helix to both the center and end sequences. The interpretation of the role of the 3_{10}-helical conformation in these peptides has evolved with time, but remains controversial. Thus, independent studies that could clarify these issues or further restrict the analysis are needed.

Here, we focus on one variant of this class of compounds, Ac-(AAKAA)$_n$-GY-NH$_2$ ($n = 1-4$), which does not have salt bridge stabilization, yet does have reduced aggregation due to dispersion of the Lys residues around the helical wheel (Rohl & Baldwin, 1994; Rohl et al., 1992; Marqusee et al., 1989). As such, these peptides are suitable for study with FTIR and vibrational CD (VCD) techniques which require concentrations higher than those normally used for ECD. We have previously demonstrated that VCD can reliably detect formation of well-defined 3_{10}-helices in peptides (Yasui et al., 1986a,b; Yoder et al., 1995, 1997; Keiderling, 1996). VCD has also been used qualitatively to detect mixed α- and 3_{10}-helical formation (S. C. Yasui et al., unpublished; Keiderling, 1996), in peptide systems with a high 3_{10}- to α-helix ratio. However, quantification of the smaller amounts of 3_{10}-helix in globular proteins, due to more variation in their detailed secondary structures, has not yet been achieved with optical spectra (Pancoska et al., 1995). VCD may provide new insights into the ongoing fundamental discussion of the role of the 3_{10}-helix conformation in helical formation initial folding events. Our temperature and solvent variation studies demonstrate that the important conformational variable of these peptides is, in fact, their α-helical content and furthermore reveal that an intermediate in the thermal unfolding pathway, which we assign to a mixed helix−coil form, must be explicitly considered to explain the spectra that result during such a thermal transition. Bringing together these observations with those noted above requires recognition of the means by which various techniques sense secondary structure, as will be addressed in the Discussion.

MATERIALS AND METHODS

Synthesis. The peptides Ac-(AAKAA)$_n$-GY-NH$_2$ ($n = 1-4$) were prepared by solid phase synthetic techniques and very kindly provided to us by C. Rohl and R. Baldwin of Stanford University. Full details of the synthesis for these peptides will be published separately (Rohl & Baldwin, 1997).

Vibrational CD. Peptide samples were dissolved directly in both D_2O and TFE to yield concentrations of ∼5 mg/100 μL. For spectroscopic measurement, these were transferred to a demountable cell composed of two CaF_2 windows separated by a 25 μm spacer (Teflon for D_2O samples and Mylar for TFE samples). Spectral measurements for these peptides in H_2O utilized higher (∼20 mg/100 μL) concentration samples and a cell having a 6 μm Mylar spacer. These experiments only proved to be possible for the two longer oligomers in the series ($n = 3$ and 4) which remained soluble under these higher concentration conditions. A dispersive VCD instrument whose design and characteristics have been described elsewhere (Keiderling, 1981, 1990) was used to collect VCD spectra at ∼10 cm^{-1} resolution using a 10 s time constant and averaging of four scans. For the purpose of baseline correction, an identically collected solvent spectrum was subsequently subtracted from the sample spectrum. A dispersive IR absorption spectrum was measured under the same conditions for purposes of normalization of the VCD spectra to allow a uniform presentation.

For the temperature variation study, the samples in D_2O were placed in a homemade variable-temperature cell consisting of two CaF_2 windows separated by a 25 μm thick Teflon spacer and contained in a small brass mount, which incorporated two O-ring seals for inhibiting leakage (Wang, 1993). This cell was then tightly fit into a homemade double-walled brass jacket through which water was pumped from a thermostatically controlled Neslab RTE-110 water bath. The bath was regulated via a thermocouple placed in the outer jacket of the cell to achieve a constant temperature. Measurements were made at 5 °C intervals starting from 5 °C to about 50 °C, or until a consistent final spectrum was obtained.

FTIR and ECD. The IR absorption spectra were recorded using a Bio-Rad Digilab FTS-40 (FTIR) spectrometer at 4 cm^{-1} nominal resolution as the average of 1024 scans using an MCT detector. The same samples were measured under the same conditions described above. To correlate with previous studies and monitor concentration effects, ECD spectra were measured in the far-UV range on solutions of these peptides at various concentrations in H_2O using quartz cells and a JASCO J-600 spectropolarimeter. A temperature variation study of a 1 mg/mL (∼0.7 mM) sample of the 17mer was carried out.

Factor Analysis. The VCD, FTIR, and ECD spectra as a function of temperature and chain length were decomposed into a linear combination of subspectra (principal components) using factor analysis (FA) (Malinowski & Howery, 1980) which is the basis of most of our protein spectra-based secondary structure analyses that have been thoroughly

detailed in the literature (Pancoska et al., 1991, 1994, 1995; Pancoska & Keiderling, 1991; Baumruk et al., 1993). The variation of the component loadings (subspectral expansion coefficients) with temperature was used to monitor the full spectral variation that accompanies any structural transitions. Mathematically, these orthogonal components (subspectra), $\phi_j(\nu)$, are obtained by projection from the set of experimental spectra, $\Theta_i(\nu)$, by using the matrix of eigenvectors resulting from diagonalization of the correlation matrix of the input spectra used in the analysis. When subspectra are combined via the coefficient (or loadings) matrix, $\mathbf{C}_{ij}$, the result represents the original experimental spectral set as

$$\Theta_i(\nu) = [\phi_j(\nu)]\mathbf{C}_{ij} \quad (1)$$

By organizing the subspectra in order of their decreasing contributions to the overall spectral variance (as quantified by the corresponding eigenvalues), we can reduce the number (z) of significant subspectra to just those components needed to describe the spectral band shape variation in the data set. This process is mathematically equivalent to finding the rank of the matrix $[\Theta_i(\nu)]$ or to determining the number of linearly independent subspectral components needed to reconstruct the experimental spectra while preferentially eliminating the random noise. We have typically used the criterion that the number (z) of subspectra retained for the analysis should be sufficient to describe 98−99% of the total spectral variance. Ideally, the number of significant subspectra found indicates the number of detectable independent structural components in the conformational mixture making up the spectra studied (Johnson, 1985).

RESULTS

IR Absorption. FTIR absorption spectra were measured over the amide I and II regions for Ac-$(AAKAA)_n$-GY-NH_2 (n = 1−4) in TFE and (n = 3 and 4) in H_2O at 25 °C and (n = 1−4) in D_2O for a range of temperatures. It is important to measure both the amide I and II modes to establish a 3_{10}-helical conformation with VCD and to compare those spectra to FTIR. The reference base of VCD for peptide structures is for samples in nonaqueous solution, so the spectra of the Ac-$(AAKAA)_n$-GY-NH_2 series in TFE provide a starting reference point. The H_2O data, more relevant to questions at hand, while limited to only the 22mer and the 17mer, primarily differ from the TFE result in the amide I frequencies, which are shifted down considerably from TFE values (∼1655 cm^{-1}), to 1643 and 1645 cm^{-1} for the 22mer and 17mer, respectively (see Discussion and Figures 1 and 2). The shoulder at ∼1672−1678 cm^{-1} in both solvents is due to residual TFA from the peptide synthesis and purification.

In D_2O, at 5 °C, both the 22mer and the 17mer display amide I′ maxima which are somewhat broader (than those in H_2O) and are found at ∼1637 cm^{-1} (Figure 3), a value which is much lower than the expected value for α-helical structures in proteins (Byler & Susi, 1986; Surewicz et al., 1993). This result is in good agreement with previous FTIR studies of highly helical, Ala-rich peptides in D_2O (Williams et al., 1996; Martinez & Millhauser, 1995; Miick et al., 1992, 1995). At shorter oligomer chain lengths, a shift up in frequency is observed, and for the 22mer and 17mer, amide I′ frequencies remain constant to ∼30 and 20 °C, respectively, whereupon they broaden and steadily shift up to 1643 cm^{-1}. The two smaller oligomers in the series (n = 1 and 2) display amide I′ frequencies at ∼1643 cm^{-1}, even at low temperatures.

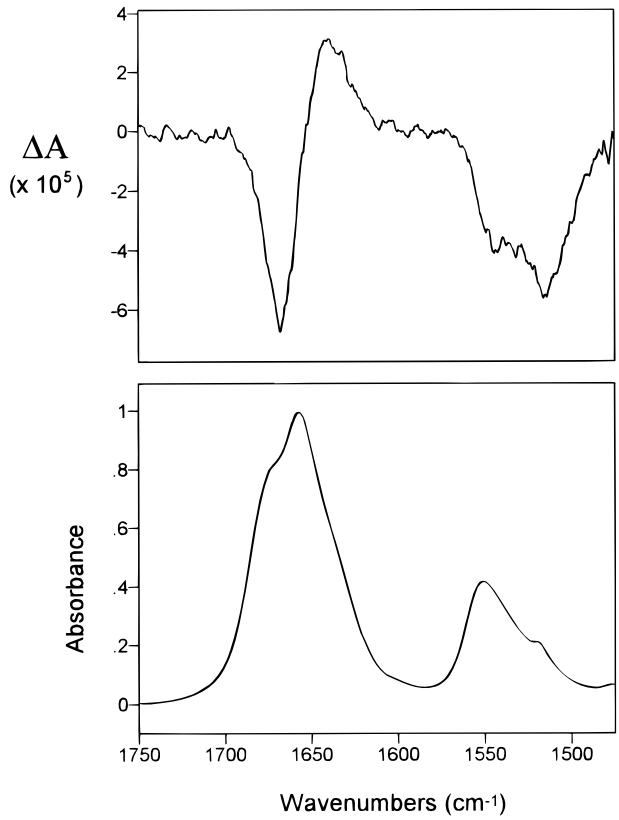

FIGURE 1: Amide I and amide II VCD (top) and FTIR (bottom) spectra for Ac-$(AAKAA)_n$-GY-NH_4 in TFE.

Vibrational Circular Dichroism. The dispersive VCD and IR absorption spectra over the amide I and II region for Ac-$(AAKAA)_n$-GY-NH_2 (just n = 4) in TFE and (n = 3 and 4) in H_2O at 25 °C are shown in Figures 1 and 2, respectively. For the sake of comparison, all VCD spectra were normalized so that the corresponding IR spectra had a peak absorbance of 1.0 for the amide I. This method offers an approximate normalization of the VCD for peptide content and is functionally more precise than the concentration and path length determinations we are able to make under these small sample, short path conditions.

The amide I VCD of the 22mer in TFE has a positive couplet shape and negative bias, and the broad negative amide II VCD is shifted to lower frequency from the absorption (Figure 1), closely matching previously observed spectra for α-helical (NH-protonated) peptides in nonaqueous environments (Yasui et al., 1987a,b; Singh & Keiderling, 1981; Sen & Keiderling, 1984; Lal & Nafie, 1982; Yasui & Keiderling, 1986a). Both the intensities and shapes of these bands remain fairly uniform for the 17mer and 12mer peptides (n = 3 and 2) in TFE. For the heptamer, the VCD pattern changes, losing most of the amide I positive lobe intensity and shifting the amide II to ∼1530 cm^{-1}, indicating some significant residual structure. Quantitatively, the VCD intensities of the n = 2, 3, and 4 oligomers in TFE are weaker (by about a factor of 2) compared to those of poly(γ-benzyl-L-glutamate) (Singh & Keiderling, 1981), a high-persistence length α-helical polypeptide, and even weaker than that for $(Met_2Leu)_6$, a helical oligomer which has a similar broad VCD band shape in $CDCl_3$ (Yasui et al., 1987a), indicating

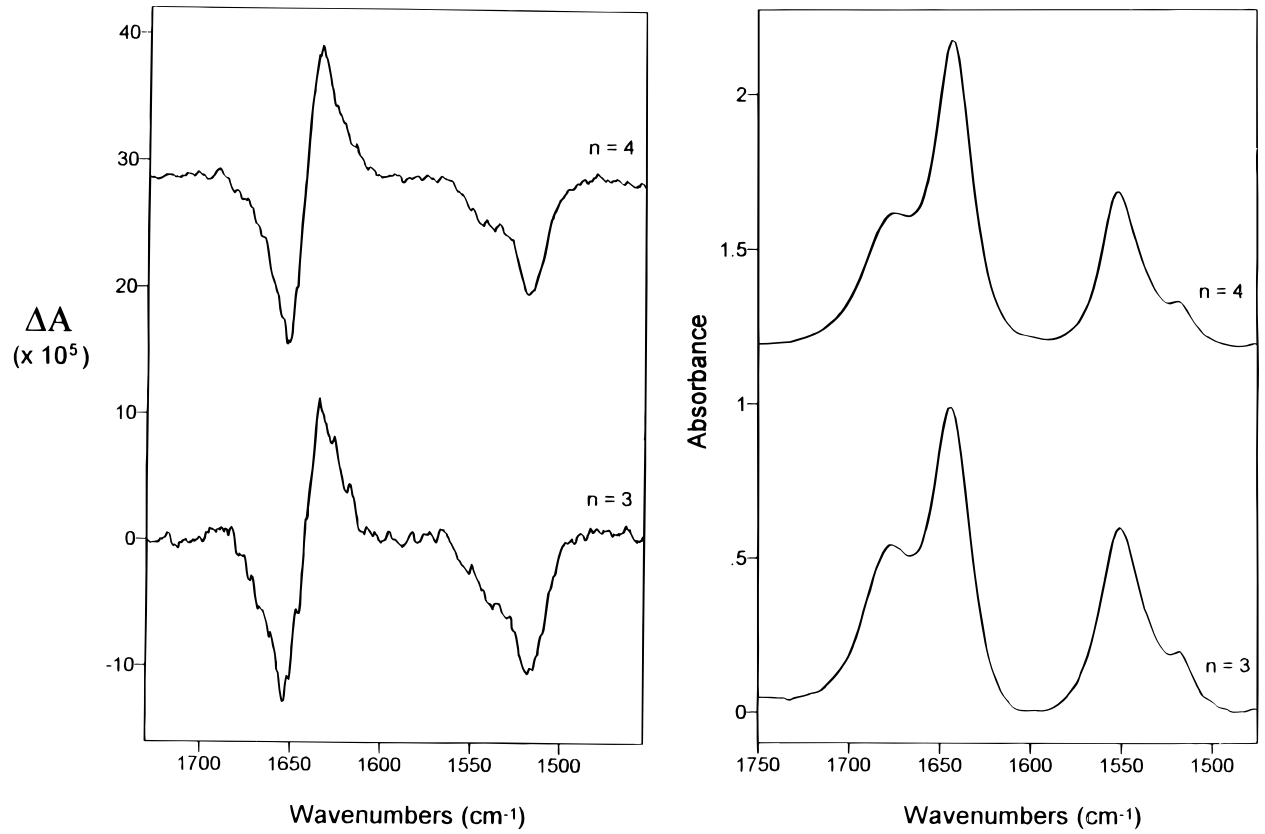

FIGURE 2: Amide I and amide II VCD (left) and FTIR (right) spectra for the peptides Ac-(AAKAA)$_n$-GY-NH$_2$ (n = 3 and 4) in H_2O.

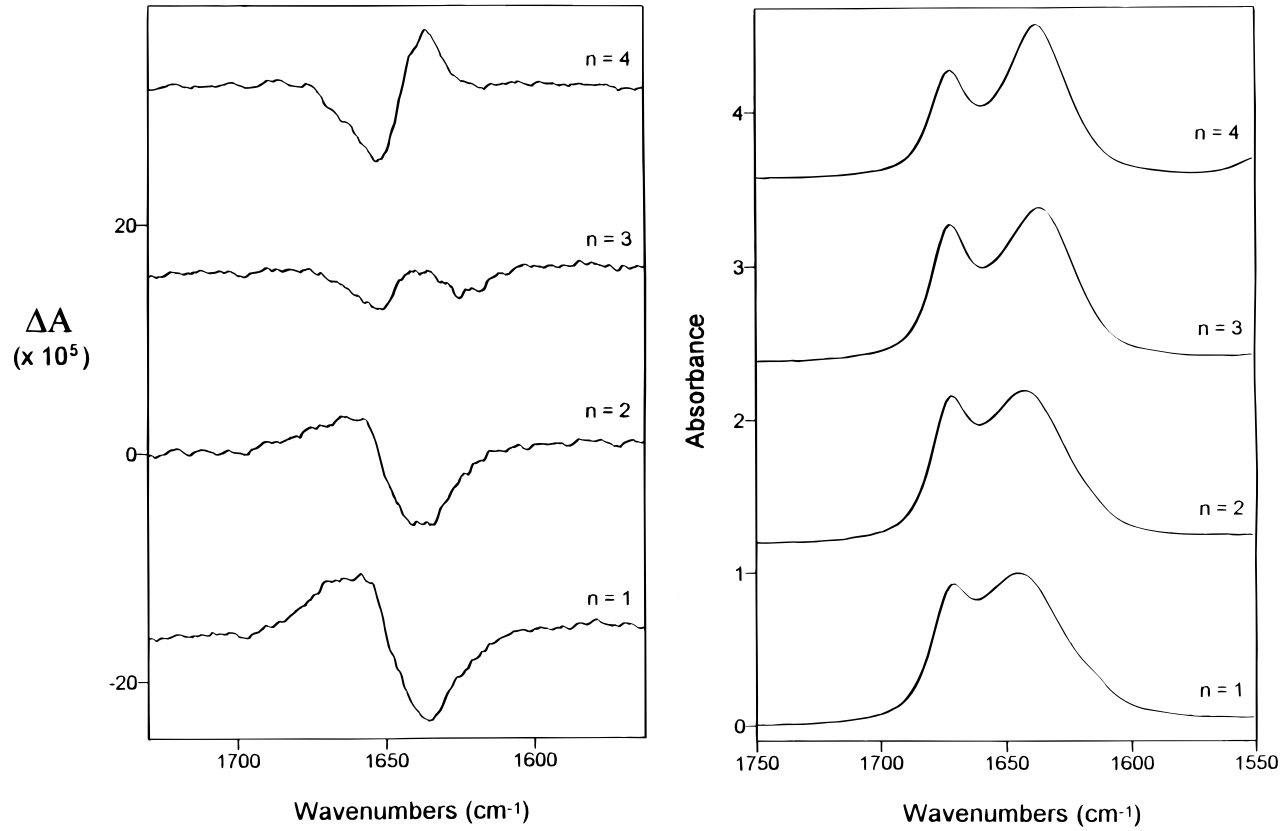

FIGURE 3: Amide I′ VCD (left) and FTIR (right) spectra at 5 °C for the peptide series Ac-(AAKAA)$_n$-GY-NH$_2$ (n = 1−4) in D_2O.

less stability for the Ala-rich peptides in TFE than for these model peptides.

The amide I and II VCD intensities and band shapes relative to their absorption bands are critical for distinguishing α- and 3_{10}-helical conformations. This requires the study of H_2O-based solutions which are restricted to very high concentrations for reasonable S/N VCD (Baumruk & Keiderling, 1993). In H_2O, the amide I VCD bands for both the n = 3 and 4 peptides (Figure 2) appear to be nearly conservative positive couplets, negative to higher energy, and have a

somewhat narrower band shape than those for the TFE result. These spectra have the same shape, but are sharper and more intense than VCD spectra obtained for several highly helical proteins in H_2O (Baumruk & Keiderling, 1993) but are similar to spectra obtained for highly helical glucoamylase in H_2O (Urbanova et al., 1993). As seen in the FTIR, the amide II bands are sharper than those seen in TFE solutions but have most of their VCD intensity in the lower-frequency component ($\sim$1520 cm^{-1}), which is opposite the FTIR intensity distribution and is distinctly characteristic of an α-helical conformation (Singh & Keiderling, 1981; Sen & Keiderling, 1989; Gupta & Keiderling, 1992). Quantitatively, the amide I VCD in H_2O is nearly twice as intense, in terms of $\Delta A/A$, as seen in TFE for both peptides. The amide II intensity is relatively high compared to that of other α-helical peptides, but is still substantially weaker than the amide I VCD, and the frequency position of its negative extreme is shifted down significantly from the absorbance maximum.

For the study of lower-concentration aqueous solutions, IR absorption and VCD spectra for each peptide in the series were measured at 5 °C in D_2O (Figure 3) for the amide I′ band (N-deuterated). The more dilute samples possible with D_2O permit reversible temperature variation, but H−D exchange of most residues (Rohl & Baldwin, 1994) shifts the amide II′ out of this region so that it is no longer a useful diagnostic. These 5 °C VCD spectra in D_2O vary from having a band shape (negatively biased positive couplet) typical of a highly helical form ($n = 4$) to one (a three-lobed w-shaped VCD pattern) indicating a mixed helix and coil structure ($n = 3$) to ones (negative couplet) mainly a characteristic of a coiled structure ($n = 2$ and 1).

The thermally induced unfolding of the alanine-rich peptide series, Ac-$(AAKAA)_n$-GY-NH_2 ($n = 4$ and 3), in D_2O was studied with VCD and FTIR, measured in 5 °C increments, and the results are summarized by only selected example VCD spectra for the 22mer in Figure 4. The amide I′ absorbances maintain a relatively consistent band shape and a slight upward shift in frequency as temperature is increased (Yoder, 1997, not reproduced here), much as is seen in Figure 3 in going from longer to shorter peptides. As seen in Figure 4, above 10 °C, the VCD band shape for the $n = 4$ peptide quickly transforms to a w-shaped profile, which gradually transforms between 35 and 45 °C to a very broad, negatively biased negative couplet that is most likely characteristic of a disordered or coil structure (Dukor, 1991; Baumruk et al., 1994; Yasui & Keiderling, 1986b; Paterlini et al., 1986). The data for the 17mer (Yoder, 1997, not presented) have the same trend as those of the 22mer, except that the initial band shape at 5 °C is a w-shaped spectrum (Figure 3) similar to the 25 °C result for the 22mer, and becomes fully changed to a negative couplet by 35 °C (Yoder, 1997, not presented). Since the shorter peptides ($n = 1$ and 2) already gave a negative VCD couplet (Figure 3) at 5 °C, their temperature variation was not studied further.

Factor Analysis. The principal component method of factor analysis (PC/FA) as adapted by us (Pancoska et al., 1979, 1991, 1994, 1995; Pancoska & Keiderling, 1991; Baumruk et al., 1996) was applied to the amide I′ (D_2O) VCD and FTIR thermal unfolding data. The goal of PC/FA application in this study is to identify those subspectral components that represent the major, thermally dependent band shape variances in our data set. This method can often allow determination of the number of independent components in a mixture, but will not necessarily provide their detailed identification. Three and two orthogonal components for the VCD were needed to reproduce the sets of temperature-dependent experimental spectra for the $n = 4$ (22mer) and $n = 3$ (17mer) oligopeptides, respectively. These subspectral components are plotted with their correct relative intensities in Figure 5 (the third subspectrum for the $n = 3$ set is shown to emphasize its insignificance). To test if the spectral variances seen with the 22mer and 17mer were independent or represented the same basic change from an altered starting point, a combined analysis was also carried out from which the resultant first and second subspectra are qualitatively similar to those found with the separate analyses. The thermal behavior of the loadings for the separate analyses is better behaved and is thus presented here, but the similarity of the two and the lack of any additional principal components confirm that the spectra of both peptides monitor the same process. The VCD band shapes observed for the data set are described primarily by the first two subspectra whose intensities are the most dominant in the group, but the third subspectrum is significant and is definitely needed to fully fit the $n = 4$, 22mer, data. This has important structural consequences.

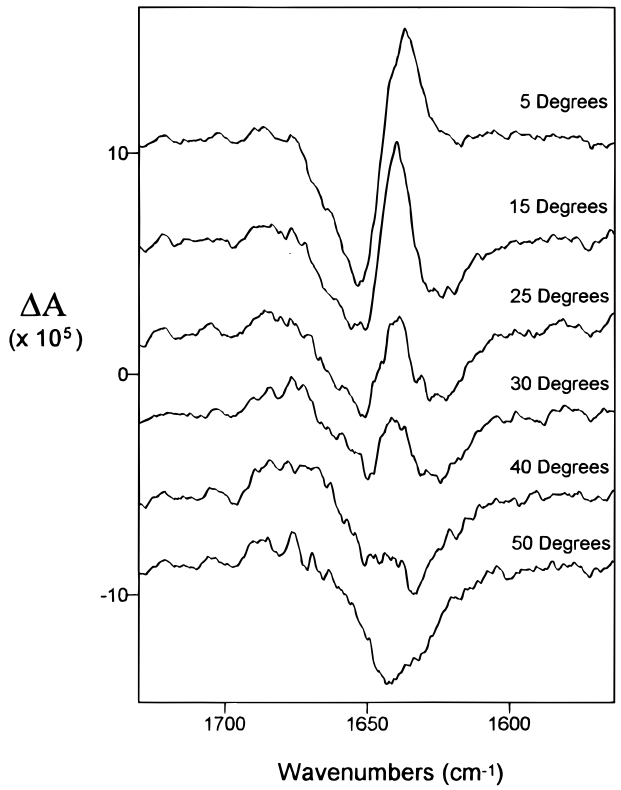

FIGURE 4: Amide I′ VCD spectra for Ac-$(AAKAA)_4$-GY-NH_2 in D_2O as a function of temperature from 5 to 50 °C.

As illustrated in Figure 6, in the separate $n = 3$ and 4 analyses, the contribution of the first subspectrum remains steady in each throughout the measured temperature range. The contribution of the second subspectrum, which has a positive couplet pattern, has the greatest variation (nearly linear decrease) over the temperature range studied. For the 22mer, the midpoint temperature for this broad transition is about 25 °C if we assume that the $T = 5$ °C state is the maximally formed helix for this oligomer in water.

For the $n = 3$ series, a similar, nearly linear variation of the coefficient of the second subspectrum with temperature

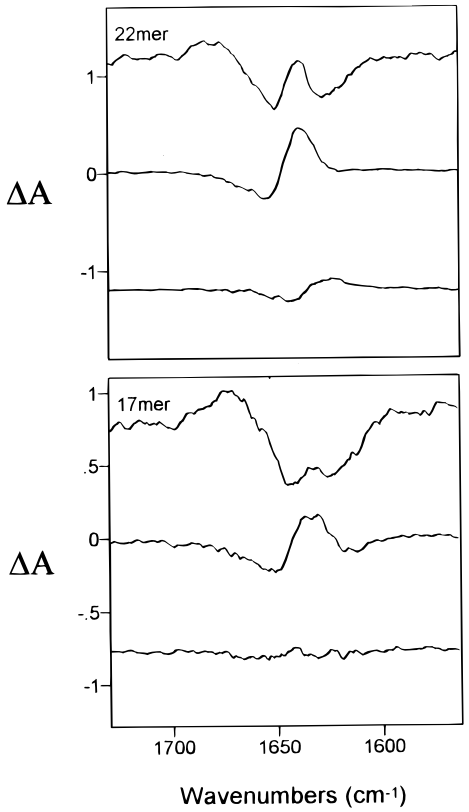

FIGURE 5: Three most significant factor analysis-derived VCD subspectra for the temperature-dependent $n = 4$ (top) and $n = 3$ (bottom) peptides Ac-(AAKAA)$_n$-GY-NH$_2$ ($n = 4$ and 3) in D_2O. Higher subspectra were representative of noise components, such as no. 3 for $n = 3$ (17 mer, bottom).

is also the largest variance. The midpoint transition temperature for $n = 3$ is more difficult to assess, at minimum lacking a stable initial state, but probably is close to 15 °C.

As we (Baumruk et al., 1996; Wi et al., 1997) and others (Williams et al., 1996; Fabian et al., 1996) have noted, representing the FTIR as difference spectra enhances the detectability of the variance in temperature-dependent absorption spectra. For this purpose, an average FTIR spectrum was calculated using the sum of all FTIR data measured within the specified temperature range. A set of difference spectra was created by subtracting the average FTIR spectrum from each individual spectrum.

For the 22mer, factor analysis of the difference spectra yields two major subspectral components with the others being reduced in intensity by at least 1 order of magnitude (Yoder, 1997, not presented). The first subspectrum, which had a strong couplet shape (corresponding to a frequency shift), exhibits the largest variation in contribution over this temperature range (Figure 6). The second subspectrum contribution varies from positive to negative and back to positive with an increase in temperature. These two temperature variations mimic those of the second and third subspectral loadings for the 22mer VCD spectra.

FA of the temperature-dependent ECD spectra of the 17mer (~1 mg/mL in H_2O) from 1 to 50 °C yielded two significant components, the first of which had slowly decreasing loadings, while the second had a much faster increase ($T_m \sim 15-20$ °C), much like that seen for the second component loading in VCD (Yoder, 1997, data not presented).

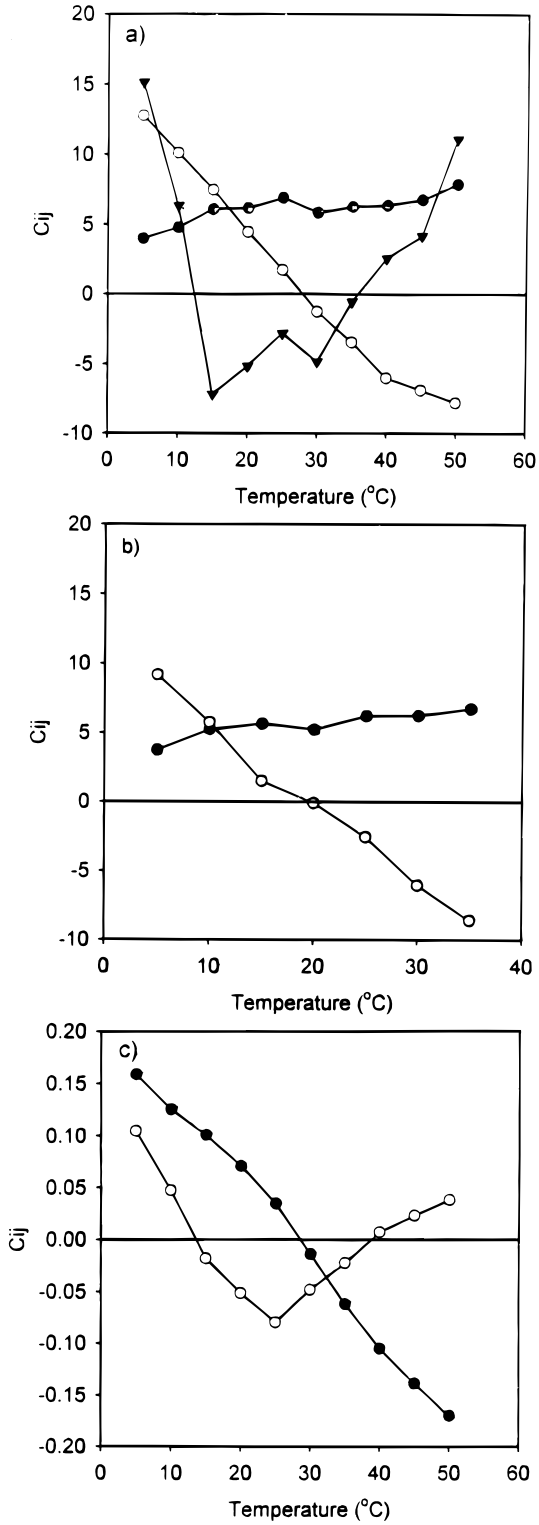

FIGURE 6: Plot of subspectral loadings $\mathbf{C}_{ij}$ as derived from factor analysis for (a) VCD subspectra 1−3 of the $n = 4$ peptide, (b) subspectra 1 and 2 of the $n = 3$ peptide, and (c) difference FTIR subspectra 1 and 2 of the $n = 4$ peptide for Ac-(AAKAA)$_n$-GY-NH$_2$ in D_2O as a function of temperature (subspectra 1, solid circles; subspectra 2, open circles; and subspectra 3, solid triangles).

DISCUSSION

Our combined studies of the VCD and FTIR spectra of Ac-(AAKAA)$_n$-GY-NH$_2$ ($n = 1-4$) in TFE, H_2O, and D_2O first lead to some conclusions in regard to the low-temperature structure of this peptide which has been the topic of some controversy. Additionally, the temperature variation study in D_2O suggests an intermediate in the thermal

denaturation of the longer oligomers studied which reflects on the probable mechanism for the unfolding of a helix. These observations address some outstanding questions noted at the outset of this project which are discussed in the sections below.

Low-Temperature Structure. The dominant structural form for the longer examples of these peptides at low temperatures is clearly α-helical. This helical form is made more complete by TFE addition, low temperatures, increased peptide lengths, and increased concentrations in aqueous environments. In TFE, the amide I shifts up and the amide II shifts down in frequency as the chain length of these peptides decreases which could correlate with a reduction in the hydrogen bond strength as well as with a decrease in the helical fraction. This pattern is also evident in D_2O, correlating with the loss of the helical fraction. Because we were able to make VCD measurements comparing the amide I′ of N-deuterated (D_2O) samples with the amide I and II of N-protonated (H_2O and TFE) ones in both aqueous and nonaqueous environments, and compare that data to FTIR and ECD for similar samples in a variety of conditions, we can confidently conclude that these spectral data yield no evidence for an extended 3_{10}-helical conformer in either the 22mer ($n = 4$) or the 17mer ($n = 3$). This confidence is based both on a comparison of band shapes with previous model compound spectra (Yasui et al., 1986a,b; Yoder et al., 1995a,b, 1997) and on the VCD intensities in terms of $\Delta A/A$. Measurements based on FTIR (Williams et al., 1996; Miick et al., 1992, 1995; Martinez & Millhauser, 1995) could not distinguish between these forms. In particular, early arguments (Miick et al., 1992) suggesting that the low amide I′ frequency found for these peptides was indicative of 3_{10}-helix formation reflect a misinterpretation of the IR frequency shifts (Martinez & Millhauser, 1995). Use of VCD band shapes avoids such assignment ambiguities (Pancoska et al., 1993; Dukor et al., 1992).

The early suggestion that for a spin-labeled 16mer "the more likely peptide geometry is a 3_{10}-helix" (Miick et al., 1992) must be viewed as being inconsistent with our VCD and FTIR data in concentrated solution as well as with all the ECD data we and others have obtained under dilute conditions (Yoder, 1997; Miick et al., 1992; Fiori et al., 1993; Marqusee & Baldwin, 1989). As noted in the introductory section, in more recent work, this interpretation has been altered to one supporting a mix of α- and 3_{10}-helix (Millhauser, 1995) and, with the latest NMR study (Millhauser et al., 1997), a proposal for a lower bound to the component of 3_{10}-helix. We again find no evidence of such a mixture, but it is important to realize that the sensitivity of optical techniques for a mixed structure is probably limited. From a simulation exercise that computationally summed the VCD band shape obtained with α-helical $(Met_2Leu)_6$ (Yasui et al., 1987a) with that of 3_{10}-helical (αMe)Val_8 (Yoder et al., 1997b), both nonaqueous, it appeared that 30% 3_{10}-helix in 70% α-helix (i.e. 0% coil) might be detectable by VCD. However, there are numerous problems in comparing such idealized spectra to real data due to solvent and αMe substitution effects on the IR frequencies and band shapes.

For comparison to the dilute conditions used for the ESR studies (Miick et al., 1992; Millhauser, 1995), ECD should be a suitable method. The issue of whether ECD is a reliable diagnostic tool for the discrimination between 3_{10}- and α-helical character in biomolecules has not been fully resolved (Sudha et al., 1983). An experimental realization of an ECD band shape discrimination between α- and 3_{10}-helical conformations, originally suggested by theoretical calculations of Manning and Woody (1991), has recently been proposed by Toniolo et al. (1996). The ratio of ellipticities at 222 and 208 nm ($R = \theta_{222}/\theta_{208}$) is used as a diagnostic, with α-helices having an R of ∼1 and 3_{10}-helices having an R of ≪1. In most cases, known 3_{10}-helical molecules have an R of <1. Our ECD studies of the (αMe)-Val_8 octapeptide concentration dependence in TFE indicated the 3_{10}-helical ECD band shape was, in fact, stabilized at high concentrations (Yoder et al., 1997), but studies of selected $(Aib\text{-}Ala)_n$ oligomers had no such dependence (Silva and Keiderling, unpublished results). Yokum et al. (1997) have shown interconvertability of these ECD band shapes upon variation between 3_{10}- and α-helix induced by amphipathic interaction with aqueous submicellar SDS.

If we assume that the proposed 3_{10}-helical ECD band shape of Toniolo et al. (1996) is appropriate for these $(AAKAA)_n$-type molecules, the published ECD results of the intermediate length peptides and also those for longer peptides seen at higher temperatures are indeterminant. At low temperatures, all of these longer peptides have ECD spectra with an R of ∼1 (Marqusee et al., 1989; Scholtz et al., 1991a,b; Fiori et al., 1993; Miick et al., 1992; Todd & Millhauser, 1991) which favors a dominant α-helical conformation. Concentration-dependent ECD for Ala-rich peptides was studied by Marqusee et al. (1989) up to 80 μM, and we have now extended that to the millimolar range for the 17mer peptide. All low-temperature ECD we have measured for the 17mer give typical qualitative α-helical band shapes (Toniolo et al., 1996) as seen for the lower concentration (Marqusee et al., 1989). Even under our most concentrated IR and VCD measurement conditions, the room-temperature ECD has a band shape close to that of the dilute sample (Yoder, 1997). But at high temperatures, our 17mer (Yoder, 1997) as well as other Ala-rich peptides has ECD with an R of <1, which can result from a mix of coil and helix forms (Andersen et al., 1996; Brown & Klee, 1971) as well as from partial 3_{10}-helical formation (Toniolo et al., 1996; Yoder et al., 1997). Shorter peptides also have an R of <1 even at lower temperatures.

Two difficulties of using ECD alone for α- vs 3_{10}-helix determination become apparent. First, the added coil component can partially diminish the strong positive ECD from an α-helix at ∼195 nm, as well as contribute to the negative ECD above 200 nm. The latter can cause an apparent decrease in R. Normalization errors of ECD instruments for a λ of <200 nm when light levels are low can also cause a nonlinear response. Second, the frequencies and intensities of these transitions are somewhat dependent on side chains and solvents (Woody & Dunker, 1996). Thus, while ECD cannot definitively settle the 3_{10}- vs α-helical question, it does imply that the low-temperature structures are most probably α-helical and that the concentration difference between EPR and VCD conditions does not induce any major structural variations.

Thermal Denaturation. The suggestion (Millhauser, 1995; Miick et al., 1995; Fiori et al., 1993) that a 3_{10}-helical intermediate or a mixed 3_{10}-helical/α-helical intermediate occurs as temperature is varied is more difficult to test and remains an open question, but is indirectly addressed by our data. The ECD data in the literature can be fully explained as a helix−coil transition, but are inconclusive with regard

to helix type. FA of the temperature-dependent ECD of the 17mer is also satisfactorily fit with two components, one having a pattern which could be consistent with either a 3_{10}- or α-helical conformation and the other with a random coil pattern (Yoder, 1997). Two components explain the 17mer changes, but are more helix selective. By contrast, FA of the VCD and FTIR temperature dependence of the 22mer demonstrates that the mechanism involves two steps, the first involving an α-helix to mixed coil−helix and the second a mixed to coil transition. This is not a solely VCD property since the variance of the first FTIR subspectral loading closely parallels that seen for the second VCD subspectrum (Figure 6).[2] Also, the loadings for the second difference FTIR subspectrum vary as seen in the third VCD subspectrum.

A comparison of the $n = 3$ and 4 results suggests both peptides unfold by the same mechanism. It is quite clear that the low-temperature 17mer ($n = 3$) form (Figure 3) is analogous in spectral band shape, and thus presumably in secondary structure distribution, to the midtemperature (∼25 °C) $n = 4$ result (Figure 4). That both thermal variations can be simultaneously analyzed with only three subspectra (Yoder, 1997) and that the separate FAs yield similarly shaped subspectra for both sets of data strongly suggest that both peptides follow the same unfolding mechanisms, but obviously start from different initial states. The second VCD subspectrum is essentially the same shape (α-helical) for both peptides, and provides the largest contribution to the variance in the amide I′ spectral intensity over the temperature range intensity. This is inconsistent with it being due to 3_{10}-helix formation, which would have a weak amide I′ VCD (Yasui et al., 1986a). These VCD and FTIR correlations of FA component variations are consistent with their monitoring the same process in both peptides and with that process involving an intermediate structure between the low-temperature α-helix and high-temperature coil forms.[3] Thus, the FA result for the 17mer ($n = 3$) supports the qualitative band shape interpretation of the thermal transition being from a mixed α-helix−coil form (the same as the 22mer intermediate) to a coil over the range studied. Furthermore, our analysis demonstrates that this intermediate unfolding structure must be a distinct conformation (as opposed to an equilibrium mix of helix and coil molecules).

The gradual loss of helical contribution and growth of the coil contribution are apparent without any analysis just from qualitative band shape comparisons, but the presence of a contribution from an intermediate structure in these spectra requires the more objective quantitative decomposition with FA. We have some confidence in qualitatively interpreting the shapes of the low- and high-temperature forms but need FA methods to determine the distinctness of the intermediate. That the FTIR- and VCD-detected temperature variations are so similar in behavior and that both require a third subspectrum indicating formation of an intermediate conformation for the $n = 4$, 22mer, data sets strongly support these spectral changes having the same origin. Further, that these FTIR and VCD data parallel previously reported ECD data (Marqusee et al., 1989; Scholtz et al., 1993; Miick et al., 1993) as well as our remeasured temperature-dependent ECD of the 17mer (Yoder, 1997) suggests that all three techniques are measuring the same structural transition at different concentrations, but that each technique is offering different insight into its character.

Nature of the Intermediate. What such an intermediate would be is not restricted by our data, but is suggested by the overall spectral response. Based on a growing body of previous work (Miick et al., 1991, 1993; Chakrabarty et al., 1991; Rohl & Baldwin, 1994; Millhauser et al., 1997), the most logical mechanism for unfolding of the helix to a disordered form is to increase steadily the degree of fraying of the ends as the temperature is increased. The most reasonable model for a process encompasses a structurally distinct helix−coil junction which leads to spectrally distinct characteristics for both VCD and FTIR. On the other hand, the precise nature of the helix−coil junction, the number of junctions in a peptide (Pancoska et al., 1996, 1997), or, for that matter, the nature of the coil conformation (Dukor & Keiderling, 1991) cannot be precisely determined from these data (see below).

The relatively short-range length dependence of IR and VCD spectra (Yasui et al., 1986b; Dukor & Keiderling, 1991; Dukor et al., 1991; Yoder et al., 1995a, 1997) can be used to sense formation of such a short-range structure as a junction and follow its development faithfully. In addition, due to their intrinsically fast time scale, VCD and FTIR can provide sensitivity to the distribution of conformational types in a dynamically changing structure. Each element of the structure will additively contribute its own characteristic response to the overall band shape. As these structural elements vary in population, the band shape will vary, and this variance will be detectable with PC/FA methods. The behavior of the loadings of the $n = 4$ subspectra (third, VCD, and second, differential FTIR) shows a decrease as the peptide begins unfolding and an increase when the transition is complete. This down−up variation (the sign of $\mathbf{C}_{ij}$ is arbitrary) is consistent with formation of a steady state concentration of junctions during the transition.

VCD and FTIR can both sense the helix−coil junction (viewed as a distinct conformation of several residues) as a differentiable structural element contributing to the measured spectra, but they cannot resolve contributions of individual residues (Pancoska et al., 1996). In a mixed conformation, the intrinsic shape of the junction spectral contribution is hard to predict. This is because of its small size and its coupling to the segments before and after it. Thus, our FA techniques are used to provide insight into separately varying spectral components without assigning the underlying structural variations to specific parts of the molecule.

In NMR by contrast, the individual residues should yield chemical shifts, for example, that are characteristic of their local conformations and less dependent on their neighboring residues. This will make NMR more sensitive to individual ϕ and ψ angles for mixed conformations than VCD and FTIR probably are. This difference in technique sensitivity may

[2] By using the difference FTIR approach, two independent subspectra have the same implication with regard to independent conformers as do three subspectra for analysis of VCD or unmodified FTIR spectral changes. As a test of this assertion, we carried out an analysis of the "normal" FTIR and found that in this case second and third subspectra and the thermal dependence of their loadings were identical with what was obtained for the first and second subspectra from the difference FTIR data, while the first, as expected (Pancoska et al., 1991, 1994; Baumruk et al., 1996), is basically the average of the data set being analyzed.

[3] The value of the second loading for $n = 4$ plotted vs that for $n = 3$ at each temperature is a straight line with a slope of 0.94 and a correlation coefficient of 0.99.

be at the root of the differences in our interpretations and the most recent ones of Millhauser et al. (1997). The VCD of the junctions most likely reflects the fact that there are structural distortions of the segments being connected. Thus, the precise nature of the junction, as opposed to a continuous segement, is less important for VCD or FTIR than for NMR. Thus, if the junction between an α-helix and a frayed coil were 3_{10}-helical in terms of local ϕ and ψ angles, it is likely that VCD would not show a qualitative 3_{10}-helical band shape, but rather some minor distortion of the helix and coil contributions to the spectral response. However, the variation of this contribution with temperature allows its presence to still be detectable with PC/FA.[4]

The VCD spectral patterns, the parallel of $n = 3$ and 4 temperature variations, and the interpretation of the junction state as an intermediate do not support the idea that a separate 3_{10}-helical intermediate state is important (Millhauser, 1995). The FTIR frequency shift of the amide I′ (~1637 to 1643 cm^{-1}) with an increase in temperature also is consistent with helix−coil (Williams et al., 1996) and inconsistent with a 3_{10}-helical form (Miick et al., 1992). The low frequency seems to be characteristic of a fully solvated helix, as has been previously suggested to explain time-dependent temperature variation experiments on a similar peptide (Williams et al., 1996). Thus, our model for the intermediate is a peptide whose fraction of frayed end residues increases with increasing temperatures rather than an intermediate peptide structure of some definite conformation. That the central helix decreases in fraction and the frayed ends increase is reflected in the variation of the first and second FA components for the VCD. That helix is decreasing at the expense of coil is reflected in the stability of the loading of the first component.

Finally, we offer no conclusions on the structure of very short helices (Hanson et al., 1996b) which may indeed contain a 3_{10}-helical turn. However, our VCD data for them in D_2O (Figure 3) indicate a dominant coil contribution even at 5 °C, while in TFE, they probably do form a turn with frayed ends that could be like a 3_{10}-helix in the middle (Yasui et al., 1986b).

Mechanistic Implications. If the junction between an α-helical segment and a frayed end involved a 3_{10}-turn, our data could neither discriminate against nor confirm this. However, such a junction alone would not constitute a 3_{10}-helical intermediate conformation. It could however represent a mechanistic step for the local residue by residue unfolding from α-helix to random coil. Our data do suggest that in such a mechanism the role of the 3_{10}-conformation is better viewed as an extension of the chain while maintaining some inter-residue hydrogen bonding rather than as the formation of a new helical form. Thus, the model might more accurately be put forth as chain propagation of α-helix to extended (3_{10}-like) turn to random coil. This is not inconsistent with the recent NMR results of Millhauser et al. (1997) in that this junction, if it were 3_{10}-like, could give rise to the intermediate NOEs found. That the NOEs are evidence of 3_{10} character for the central residues can be thought to suggest that the peptide is relatively unstable, sampling various unfolded conformers even at low temperatures.

With the intermediate and its nature established to the extent possible with optical spectra, one can discuss its impact on the numerous efforts to use such data to determine thermodynamic and kinetic parameters. Many of the thermodynamic studies based on Lifson-Roig (1961) or Zimm and Bragg (1959) theory seek to model the conversion between conformers as each residue having either helix or coil conformational parameters (Scholtz et al., 1991a,b). However, CD or even FTIR does not sense such local structural parameters directly. Thus, the assumption that such a correlation *a priori* would be valid is a large one. That such modeling of ECD data with such assumptions does work so well might be viewed either as a coincidence or, more realistically, as being due to the particular structural sensitivities of ECD. Peptide ECD is primarily sensitive to long-range dipole coupling of the amides which in general depends on the stereochemistry of several residues along the chain. VCD has shorter range sensitivity, but still is affected by the conformations of the residues making up a turn of the helix (or coil) (Keiderling, 1996; Dukor & Keiderling, 1991). IR in turn depends on hydrogen bonding (a few residues away) as well as local dihedral angles. Thus, while all of these techniques will sense both the helix and coil components of the frayed intermediate, the vibrational spectroscopic measurements will be more significantly affected by the specific junctions and the interactions across them (Pancoska et al., 1996). In an oligopeptide, such contributions are not negligible, and due to the intrinsically fast time scale of optical spectra, all dynamically accessed conformers will contribute to the observed result.

Similarly, as recognized by Williams et al. (1996), using an equilibrium constant to determine a reverse kinetic pathway depends on microscopic reversibility. In the presence of a definite intermediate state, interpreting the value obtained as the rate constant for folding a helix from a fully unfolded state is dangerous. At best, one might be measuring a rate from a partially folded (helix already initiated) to a more fully folded form which would be a helix propagation rate rather than a folding rate. In our suggested model, this would be a sequential change for specific residues from a helical to an extended turn to a coil character.[5] Previous studies have indicated a difference between thermal- and chemical-induced unfolding of these peptides (Miick et al., 1993). The thermal "unfolded" state may well be a distribution of local structures with a significant population of "extended helices" which have been interpreted to be characterized by a left-handed twist (Dukor & Keiderling, 1991). That it also might locally sample 3_{10}-helical forms is reasonable (Millhauser, 1995).

While few would be surprised that TFE stabilized the helical form, another observation we have made, albeit

[4] The fact that the VCD and FTIR temperature variations are both sensitive to the presence of such junctions gives strong empirical support for the extensions of analyses of optical spectra beyond evaluation of just the traditional fractional secondary structure, for utilizing this junction sensitivity for enumeration of segments of secondary structure (Pancoska et al., 1994, 1996, 1997). That it should be possible to detect components of a structure without establishing their isolated contributions to a spectrum logically follows from the use of these techniques to detect turns in globular proteins without assigning them a unique band shape (Pancoska et al., 1996; Wi et al., 1997).

[5] The ~20 °C temperature jump used in these studies (Williams et al., 1996) would leave the junction concentration roughly constant. The observable conformational change would be just between the populations of helix and coil, a pseudo-two-state problem.

somewhat indirectly, is that these α-helical structures are stabilized by peptide−peptide interaction. This is suggested by comparing the room-temperature H_2O data for the $n = 3$ and 4 peptides which are both predominantly helical with those obtained in a D_2O solution 4-fold more dilute where the $n = 4$ form is a mixed helix−coil structure and the $n = 3$ form almost completely coil at room temperature. ECD studies on solutions at least 1 order of magnitude more dilute certainly should not be evidence of any complications due to peptide interaction, but NMR measurements as well as these IR and VCD studies are potentially subject to them. It is interesting to note that the ECD thermal studies for these peptides are concentration-independent up to the millimolar range and qualitatively follow the VCD and FTIR results (at >10 mM) which suggests that our concentrations in D_2O are not a significant problem. It should be noted that the kinetic studies by Williams et al. (1996) used more dilute samples than our FTIR ones and a different sequence which may reduce peptide−peptide interactions in their case.

CONCLUSION

VCD and factor analysis for the alanine-rich peptide series Ac-$(AAKAA)_n$-GY-NH_2 have proven to be useful tools for monitoring the helix−coil transition as well as for characterizing helix stability. Correlation of these data with parallel FTIR and ECD studies strengthens the impact of the conclusions. Temperature as well as peptide chain length impacts the helical stability of these molecules to a very high degree. Variations in solvent composition and concentration also affect the stability of the α-helical form. This study is another example which demonstrates the ability of VCD to describe the detailed helical nature of biomolecules when other spectroscopic methods may fall short of this goal.

ACKNOWLEDGMENT

We thank warmly Dr. Carol Rohl and Professor Robert L. Baldwin of Stanford University for generously providing us with ample peptide samples so we could pursue this study and for discussion of the results and suggestions with regard to the methods used.

REFERENCES

Andersen, N. H., Liu, Z., & Prickett, K. S. (1996) *FEBS Lett. 399*, 47−52.
Baumruk, V., & Keiderling, T. A. (1993) *J. Am. Chem. Soc. 115*, 6939−6942.
Baumruk, V., Huo, D., Dukor, R. K., Keiderling, T. A., Lelievre, D., & Brack, A. (1994) *Biopolymers 34*, 1115−1121.
Baumruk, V., Pancoska, P., & Keiderling, T. A. (1996) *J. Mol. Biol. 259*, 774−790.
Bour, P., & Keiderling, T. A. (1993) *J. Am. Chem. Soc. 115*, 9602−9607.
Brown, J. E., & Klee, W. A. (1971) *Biochemistry 10*, 470−476.
Byler, D. M., & Susi, H. (1986) *Biopolymers 25*, 469−485.
Dukor, R. K., & Keiderling, T. A. (1991) *Biopolymers 31*, 1747−1761.
Dukor, R. K., Keiderling, T. A., & Gut, V. (1991) *Int. J. Pept. Protein Res. 38*, 198−203.
Dukor, R. K., Pancoska, P., Prestrelski, S., Arakawa, T., & Keiderling, T. A. (1992) *Arch. Biochem. Biophys. 298*, 678−681.
Fiori, W. R., Miick, S. M., & Millhauser, G. L. (1993) *Biochemistry 32*, 11957−11962.
Freedman, T. B., Nafie, L. A., & Keiderling, T. A. (1995) *Biopolymers 37*, 265−279.
Gupta, V. P., & Keiderling, T. A. (1992) *Biopolymers 32*, 239−248.
Hanson, P., Martinez, G., Millhauser, G., Formaggio, F., Crisma, M., & Toniolo, C. (1996a) *J. Am. Chem. Soc. 118*, 271−272.
Hanson, P., Millhauser, G., Formaggio, F., Crisma, M., & Toniolo, C. (1996b) *J. Am. Chem. Soc. 118*, 7618−7625.
Johnson, W. C. (1985) *Methods Biochem. Anal. 31*, 61−163.
Keiderling, T. A. (1981) *Appl. Spectrosc. Rev. 17*, 189−226.
Keiderling, T. A. (1990) in *Practical Fourier Transform Infrared Spectroscopy* (Ferraro, J. R., & Krishnan, K., Eds.) pp 203−284, Academic, San Diego.
Keiderling, T. A. (1996) in *Circular Dichroism and the Conformational Analysis of Biomolecules* (Fasman, G. D., Ed.) pp 555−598, Plenum, New York.
Lal, B., & Nafie, L. A. (1982) *Biopolymers 21*, 2161−2183.
Lifson, S., & Roig, A. (1961) *J. Chem. Phys. 34*, 1963−1974.
Lyu, P.-C., Marky, L. A., & Kallenbach, N. R. (1989) *J. Am. Chem. Soc. 111*, 2733−2734.
Malinowski, E. R., & Howery, D. G. (1980) *Factor Analysis in Chemistry*, Wiley, New York.
Manning, M., & Woody, R. W. (1991) *Biopolymers 31*, 569−586.
Marqusee, S., & Baldwin, R. L. (1987) *Proc. Natl. Acad. Sci. U.S.A. 84*, 8898−8902.
Marqusee, S., Robbins, V. H., & Baldwin, R. L. (1989) *Proc. Natl. Acad. Sci. U.S.A. 86*, 5286−5292.
Martinez, G., & Millhauser, G. (1995) *J. Struct. Biol. 114*, 23−27.
Merutka, G., & Stellwagen, E. (1990) *Biochemistry 29*, 894−898.
Miick, S. M., Todd, A. P., & Millhauser, G. L. (1991) *Biochemistry 30*, 9498−9503.
Miick, S. M., Martinez, G., Fiori, W. R., Todd, A. P., & Millhauser, G. L. (1992) *Nature 359*, 653−655.
Miick, S. M., Casteel, K. M., & Millhauser, G. L. (1993) *Biochemistry 32*, 8014−8021.
Miick, S. M., Martinez, G., Fiori, W. R., Todd, A. P., & Millhauser, G. L. (1995) *Nature 377*, 257.
Millhauser, G. (1995) *Biochemistry 34*, 3873−3877.
Pancoska, P., & Keiderling, T. A. (1991) *Biochemistry 30*, 6885−6895.
Pancoska, P., Fric, I., & Blaha, K. (1979) *Collect. Czech. Chem. Commun. 44*, 1296−1312.
Pancoska, P., Yasui, S. C., & Keiderling, T. A. (1989) *Biochemistry 28*, 5917−5923.
Pancoska, P., Yasui, S. C., & Keiderling, T. A. (1991) *Biochemistry 30*, 5089−5103.
Pancoska, P., Wang, L., & Keiderling, T. A. (1993) *Protein Sci. 2*, 411−419.
Pancoska, P., Bitto, E., Janota, V., & Keiderling, T. A. (1994) *Faraday Discuss. 99*, 287−310.
Pancoska, P., Bitto, E., Janota, V., Urbanova, M., Gupta, V. P., & Keiderling, T. A. (1995) *Protein Sci. 4*, 1384−1401.
Pancoska, P., Fabian, H., Yoder, G., Baumruk, V., & Keiderling, T. A. (1996) *Biochemistry 35*, 13094−13106.
Paterlini, M. G., Freedman, T. B., & Nafie, L. A. (1986) *Biopolymers 25*, 1751−1765.
Perutz, M. F., & Fermi, G. (1988) *Proteins: Struct., Funct., Genet. 4*, 294−295.
Rohl, C. A., & Baldwin, R. L. (1994) *Biochemistry 33*, 7760−7767.
Rohl, C. A., & Baldwin, R. L. (1997) *Biochemistry 36*, 8435−8442.
Rohl, C. A., Scholtz, J. M., York, E. J., Stewart, J. M., & Baldwin, R. L. (1992) *Biochemistry 31*, 1263−1269.
Scholtz, J. M., & Baldwin, R. L. (1992) *Annu. Rev. Biophys. Biomol. Struct. 21*, 95−118.
Scholtz, J. M., Qian, H., York, E. J., Stewart, J. M., & Baldwin, R. L. (1991a) *Biopolymers 31*, 1463−1470.
Scholtz, J. M., York, E. J., Stewart, J. M., & Baldwin, R. L. (1991b) *J. Am. Chem. Soc. 113*, 5102−5104.
Sen, A. C., & Keiderling, T. A. (1984) *Biopolymers 23*, 1519−1532.
Singh, R. D., & Keiderling, T. A. (1981) *Biopolymers 20*, 237−240.
Sudha, T. S., Vijayakumar, E. K. S., & Balaram, P. (1983) *Int. J. Pept. Protein Res. 22*, 464−468.
Surewicz, W., Mantsch, H. H., & Chapman, D. (1993) *Biochemistry 32*, 389−394.

Todd, A. P., & Millhauser, G. L. (1991) *Biochemistry 30*, 5515−5523.

Toniolo, C., Valente, E., Formagio, F., Crisma, M., Pilloni, G., Corraja, C., Toffoletti, A., Martinez, G. V., Hanson, M. P., Millhauser, G. L., George, C., & Flippen-Andersen, J. L. (1995) *J. Pept. Sci. 1*, 45−47.

Toniolo, C., Polese, A., Formaggio, F., Crisma, M., & Kamphuis, J. (1996) *J. Am. Chem. Soc. 118*, 2744−2745.

Urbanova, M., Pancoska, P., & Keiderling, T. A. (1993) *Biochim. Biophys. Acta 1203*, 290−294.

Venyaminov, S. Y., & Kalnin, N. N. (1990) *Biopolymers 30*, 1273−1280.

Wang, L. (1993) Ph.D. Thesis, University of Illinois at Chicago, Chicago.

Wi, S., Pancoska, P., & Keiderling, T. A. (1998) *Biospectroscopy* (in press).

Williams, S., Causgrove, T. P., Gilmanshin, R., Fang, K. S., Callender, R. H., Woodruff, W. H., & Dyer, R. B. (1996) *Biochemistry 35*, 691−697.

Woody, R. W., & Dunker, A. K. (1996) in *Circular Dichroism and the Conformational Analysis of Biomolecules* (Fasman, G. D., Ed.) pp 109−158, Plenum, New York.

Yasui, S. C., & Keiderling, T. A. (1986a) *Biopolymers 25*, 5−15.

Yasui, S. C., & Keiderling, T. A. (1986b) *J. Am. Chem. Soc. 108*, 5576−5581.

Yasui, S. C., Keiderling, T. A., Bonora, G. M., & Toniolo, C. (1986a) *Biopolymers 25*, 79−89.

Yasui, S. C., Keiderling, T. A., Formaggio, F., Bonora, G. M., & Toniolo, C. (1986b) *J. Am. Chem. Soc. 108*, 4988−4993.

Yasui, S. C., Keiderling, T. A., & Katakai, R. (1987a) *Biopolymers 26*, 1407−1412.

Yasui, S. C., Keiderling, T. A., & Sisido, M. (1987b) *Macromolecules 20*, 2403−2406.

Yoder, G., Keiderling, T. A., Crisma, M., Formaggio, F., & Toniolo, C. (1995a) *Biopolymers 35*, 103−111.

Yoder, G., Keiderling, T. A., Formaggio, F., Crisma, M., Toniolo, C., & Kamphuis, J. (1995b) *Tetrahedron Asymmetry 6*, 687−690.

Yoder, G., Keiderling, T. A., Formaggio, F., Crisma, M., Toniolo, C., & Kamphuis, J. (1997) *J. Am. Chem. Soc. 119*, 10278−10285.

Yokum, T. S., Gauthier, T. S., Hammer, R. P., & McLaughlin, M. L. (1997) *J. Am. Chem. Soc. 119*, 1167−1168.

Zimm, B. H., & Bragg, J. K. (1959) *J. Chem. Phys. 31*, 526−535.

BI971460G